Materials Research, Vol. 7, No. 2, 247-253, 2004.

Influence of Deformation on the Kinetics of Phase Transformation in a Forging Steel During Warm Working

Mauro Aparecido Ferreira de Oliveira[a], *Alberto Moreira Jorge Jr*[b], *Oscar Balancin*[b]*

[a]*SIFCO S.A., Jundiaí - SP, Brazil*
[b]*Department of Materials Engineering, Federal University of São Carlos, UFSCar*
Rod. Washington Luiz, Km 235, 13565-905 São Carlos - SP, Brazil

Received: July 24, 2003; Revised: January 18, 2004

Dilatometric techniques were used to determine the start and finish transformation heating temperatures for a carbon steel (0.30% C - 1.5% Mn). The mechanical behavior of the steel was measured by torsion testing in the temperature range of 700 to 820 °C with holding times ranging from 1 to 30 min. The flow stress curves presented different shapes and stress levels. These differences were attributed to the ferrite and pearlite, ferrite and austenite, and austenite strained structures. When ferrite and pearlite were deformed together, the flow stress presented a hump with little straining; when the austenitic structure was deformed the shape of the flow stress curve was typical of materials having low stacking fault energy. The microstructural evolution observed by optical and scanning electron microscopy revealed that the evolution of the phase transformation was dependent on the testing temperatures, holding times and amount of straining. Comparisons were made on the kinetics of phase transformation with and without the application of plastic deformation, and evidence of strain-induced dynamic transformation was investigated.

Keywords: *warm working, pearlite austenite transformation, flow stress curves*

1. Introduction

In recent years, increasing attention has been focused on steel working to improve the metallurgical features of formed parts and to produce forms as similar as possible to the net shape forms. One possible route to achieve these goals is deformation under warm working conditions, a technique that provides greater dimensional precision than hot working, moderate surface oxidation, and improved mechanical characteristics, obviating further machining and sometimes thermal treatments. However, warm working requires a more in-depth understanding of both the deformation process and the plastic behavior of materials, since this type of operation induces stronger mechanical efforts, often causing deformation in the intercritical region.

Manganese steels with a ferrite-pearlite starting microstructure are usually applied in the production of forged components. Upon heating, pearlite becomes unstable above the eutectoid temperature (AC_1), whereas primary ferrite does not revert completely to austenite except above AC_3 temperature. The formation of austenite from the ferrite-pearlite microstructure can be described as a sequence of three stages[1]. First, the pearlite regions are converted to carbon supersaturated austenite. In this step, austenite nucleates heterogeneously at the boundary of pearlite colonies and/or ferrite-pearlite interfaces[1,2,3]. Austenite nuclei in pearlite grow when carbon atoms are transported by diffusion to the ferrite/austenite boundary from the austenite/cementite boundary through austenite and from the ferrite/cementite boundary through ferrite, transforming the ferritic lattice to austenitic lattice[4]. In the second stage, the austenite/ferrite boundaries move to decrease the amount of ferrite, until the equilibrium volume fraction of austenite is reached. At high temperatures within the intercritical domain, the growth of austenite into ferrite is controlled by carbon diffusion in the austenitic phase and, at lower temperatures, by manganese diffusion in ferrite[3]. At the final step, the equilibrium of the manganese content

*e-mail: balancin@power.ufscar.br

in austenitic and ferritic phases is controlled by manganese diffusion in the austenite, which is a much slower process than in ferrite[3].

It is well known that dislocation substructures formed during deformation increase the free energy and the number of potential nucleation sites accelerating diffusional-phase transformations[5,6]. One expects that dynamic phenomena should be enhanced by deformation assisted transformations bringing about continual straining during transformation[7]. The applied deformation enhances intragranular nucleation of the new phase within the untransformed grains promoting strain-induced transformation[8,9]. This is analogous to dynamic recrystallization. In the present work the transformation of a pearlite + ferrite microstructure into austenite during warm deformation of a medium carbon steel was studied. Attention was focused on the second stage of this transformation. The microstructural evolution of the ferrite into austenite transformation was quantified, seeking for evidences of strain-induced dynamic transformation.

2. Material and Experimental Procedures

The investigated material was a commercial medium carbon vanadium microalloyed forging steel whose chemical composition is given in Table 1. To determine the continuous-heating-transformation diagram, dilatometry tests were carried out using 2 mm diameter, 12 mm long samples. These samples were heated at a rate of 1 to 10 °C/s.

Mechanical tests were carried out on a computerized hot torsion machine. The samples, having a 20 mm length and 6 mm diameter in the reduced central gage section, were heated in an infrared furnace coupled on the testing machine. Chromel-alumel thermocouples were used for measuring the temperature. Throughout the tests, argon balanced with 2% hydrogen was continuously flushed through a quartz tube surrounding the sample. This tube was also used to inject water immediately, once the required strain had been attained, in order to freeze the high-temperature microstructures for further observations. Data were collected by means of a software program that imposes parametric tests such as temperature, holding time and amount of straining.

Warm torsion tests were carried out after heating up the samples at a rate of 1.7 °C/s from room to testing temperatures (700, 720, 750, 780 and 820 °C). The specimens were held at these temperatures from 1 to 30 min and deformed at an equivalent strain rate of 1 s^{-1}. In order to correlate the amount of deformation with the microstructural evolution, two different tests were performed in this investigation. In one test, the samples were isothermally strained to fracture to determine the flow stress behavior. In the other, the tests were interrupted at selected strains and the samples were quenched by injecting water through the quartz tube immediately after deformation. After standard metallographic procedures, the microstructural evolution was observed by scanning electron and optical microscopy and the phases were quantified.

3. Results

Start and finish transformation temperatures, under continuous heating conditions determined by dilatometry tests, are illustrated in the continuous-heating-transformation diagram plotted in Fig. 1. These data indicate that the heating rate exerts a stronger influence on the finish temperature, when all the ferritic phase is exhausted, than on the start temperature at the beginning of pearlite dissolution.

To create a reference to analyze the role of the deformation in the transformation kinetics, the evolution of the volume fraction of ferrite as a function of the temperature with holding times of 0, 1, 3 and 30 min was measured in experiments conducted isothermally at 720, 750, 780 and 810 °C without any straining, as illustrated in Fig. 2. The results indicated that, regardless the holding time, no transformation of ferrite into austenite was observed to occur at 720 °C. This transformation began at 750 °C, and the tendency for the ferritic phase to be consumed increased as the tempera-

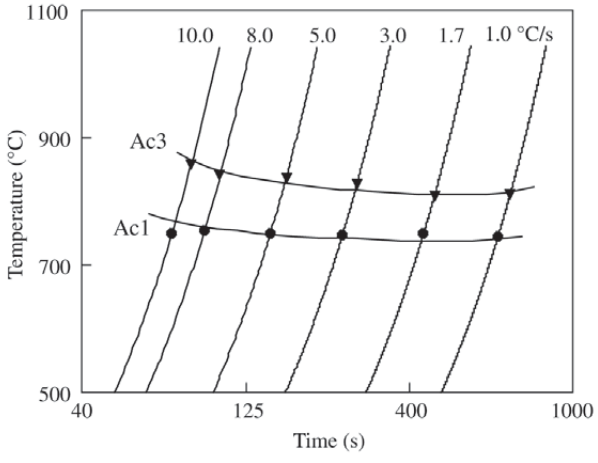

Figure 1. Continuous-heating-transformation diagram determined by dilatometry.

Table 1. Chemical composition of the tested steel (wt.%).

C	Mn	Si	P	S	Al	V	Ti	N
0.30	1.52	0.64	0.016	0.033	0.024	0.1	0.024	0.017

ture rose. The entire volume fraction of ferrite was exhausted after long holding times at 810 °C.

Figure 3 illustrates some flow stress curves determined by isothermal continuous torsion tests. These curves represent the different shapes and flow-stress levels presented by all the experiments carried out in this study. After a 1 min holding time at 700 °C, the flow curve shows a rapid work hardening to a hump, followed by an extensive flow-softening region. The peak stress (437 MPa) was reached after a slight straining (ε = 0,14). At 820 °C, the flow stress rose in the initial work-hardening regime and also reached a maximum (213 MPa) before dropping to the steady state, albeit after greater straining (ε ~ 0.5). As can be seen, all the remaining curves displayed shapes and flow-stress levels intermediate to the ones described above, and the differences were temperature and holding time-dependent.

Although the flow stress curves changed considerably, these differences were significantly higher at the beginning of the straining, in the work-hardening regime. In order to delineate this stage on the flow stress curves, the evolution of peak stress and peak strain as a function of holding times before straining was determined, as illustrated in Figs. 4 and 5. As shown in Fig. 4, the peak stress decreased continuously with the holding time, a decrease that was more noticeable at low temperatures and short holding times. In contrast, the peak strain was fairly insensitive to the holding time, but changed considerably with testing temperatures. At low temperatures, the peak strains were found below ε = 0.2 and, at higher temperatures, they exceeded ε = 0.4.

To analyze the plastic behavior at the beginning of the

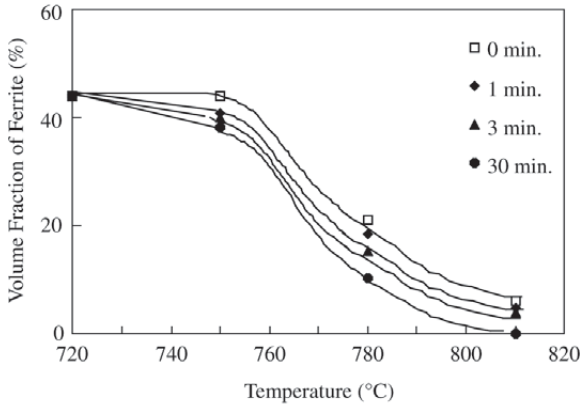

Figure 2. Evolution of the volume fraction of ferrite as a function of temperature in experiments conducted without any deformation.

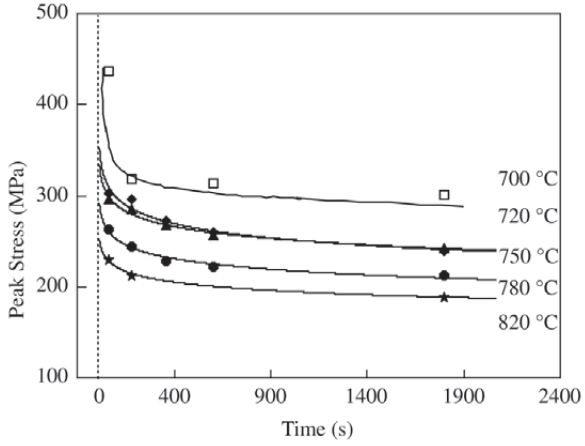

Figure 4. Dependence of the peak stress on the holding time before deformation.

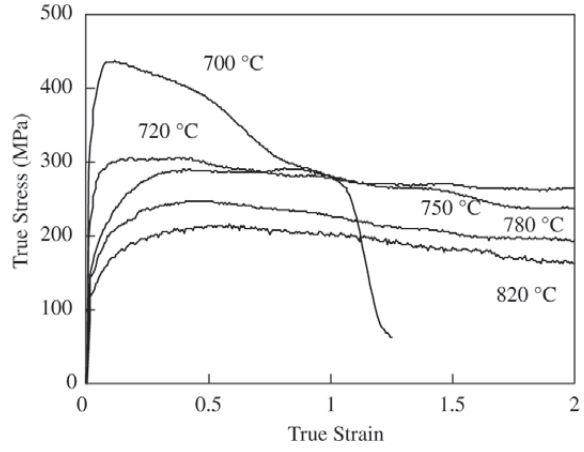

Figure 3. Continuous isothermal flow stress curves for 1 min (700 °C) and 3 min (720, 750, 780 and 820 °C) holding time.

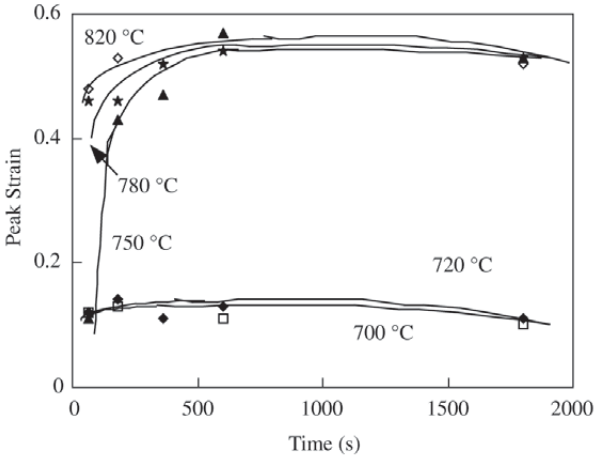

Figure 5. Dependence of the peak strain on the holding time before deformation.

deformation, the evolution of the work-hardening rate illustrated by the flow curves in Fig. 3 was calculated and is displayed in Fig. 6a as a function of the applied stress. At lower temperatures, the work-hardening rate dropped sharply as the applied stress increased to the peak stress, indicating that dynamic softening mechanisms are not effective in this region and that the plastic behavior of the material was controlled by work-hardening mechanisms. The work-hardening rate continued to drop as the deformation temperature rose. The curve still maintained a linear shape at intermediate temperatures, with milder slopes, suggesting that some dynamic softening mechanisms were active. Fig. 6b shows that the curve took on a parabolic shape at 820 °C, evidencing an inflexion point close to the peak stress. The downward deflection of the work-hardening rate resulted from the nucleation of new unstrained grains, representing the onset of the dynamic recrystallization[10,11]. In this case, the work-hardening rate displayed the characteristic shape of materials with relatively low stacking fault energy. Therefore, the flow stress curves took on the typical shape of materials that soften by dynamic recrystallization[11]. This behavior is typical of the austenitic structure during hot deformation[12].

Figures 7 and 8 show some micrographs depicting the structural evolution occurred during torsion testing. The microstructural evolution presented in the micrographs of Fig. 7 displays the first stage of the phase transformation, that is, pearlite into austenite. After heating up the sample from room temperature to 720 °C, the microstructure consisted of ferrite and pearlite. After a 3 min holding time, some austenite nuclei at the junction between pearlite colonies and ferrite-pearlite interfaces were observed (Fig. 7a). However, the evolution of the transformation during the straining was not noticeable; both the constituents were still present and were aligned in the strain direction (Fig. 7b). The growth of austenite into pearlite was observed at higher temperatures, as displayed in Fig. 7c. The microstructure of the sample reheated to 750 °C and water quenched after 1 min holding time shows austenite/ferrite interfaces growing into pearlite.

Figure 8 shows a set of micrographs displaying the second stage of the phase transformation: ferrite into austenite transformation. The micrograph of the sample strained to $\varepsilon = 0.5$ at 750 °C after a 3 min holding time reveals that ferrite and austenite were simultaneously deformed, and a dislocation substructure was formed within the ferrite phase during straining (Fig. 8a). As the deformation proceeded, the substructure acted as intragranular nucleation sites and austenite particles were nucleated in the untransformed ferrite grains, as can be seen in Fig. 8b. After higher straining, the growth of new austenite grains occurred with consequent decrease in the volume fraction of ferrite (Fig. 8c), tending toward equilibrium values. Measurements of the volume fraction of ferrite as a function of deformation, Fig. 9, confirm this statement. Also, it is worth noting in Figs. 8a and 8b that the dynamic transformation of ferrite into austenite was no longer controlled by austenite growth only, as a new process of intragranular nucleation occurred.

4. Discussion

After determining the start and finish transformation temperatures during heating, the samples were deformed within and close to the intercritical domain for different holding times. The flow stress curves displayed different

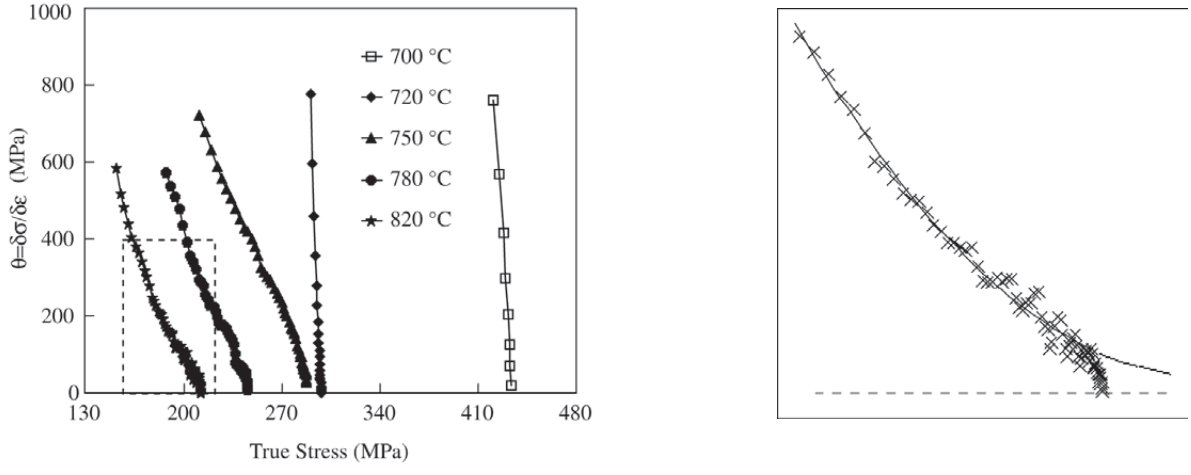

Figure 6. a) Work-hardening rate as a function of the applied stress calculated from data displayed in Fig. 3.; b) Details of the work-hardening-rate evolution for the experiment conducted at 820 °C.

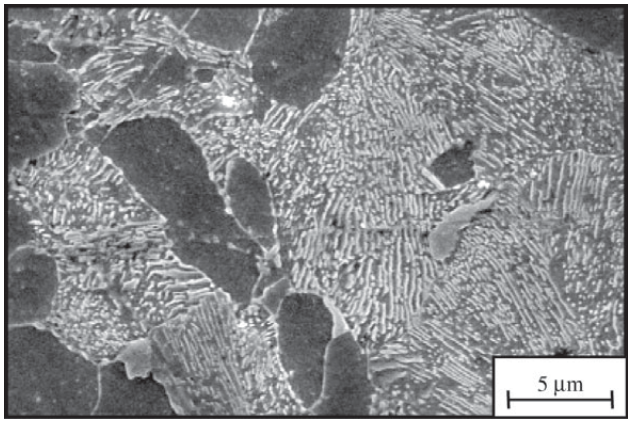

(a)

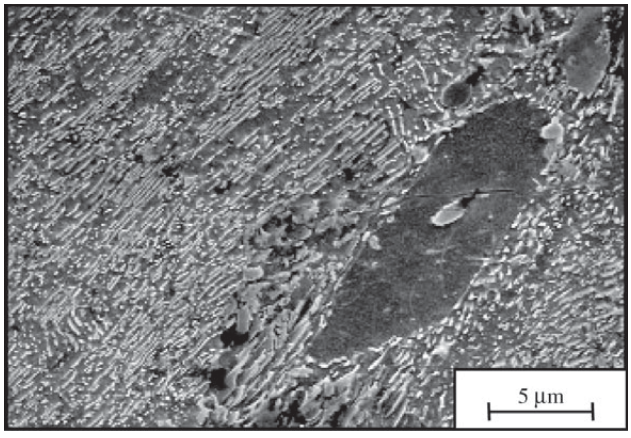

(b)

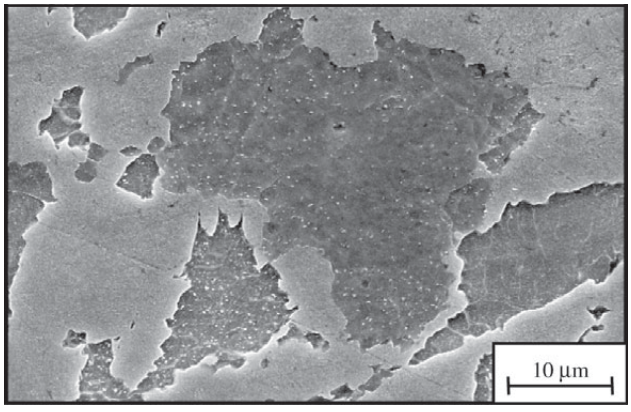

(c)

Figure 7. Microstructural evolution during the transformation of pearlite into austenite. a) Sample reheated to 720 °C and water quenched after 3 min holding time; b) Sample strained to ε = 1.5 at 720 °C after a 3 min holding time; c) Sample reheated to 750 °C and water quenched after 1 min holding time.

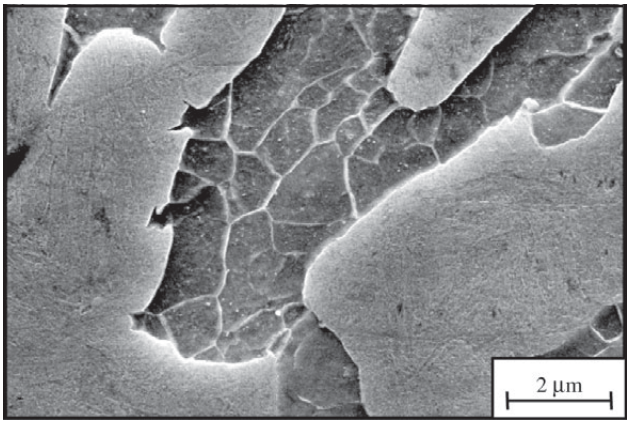

(a)

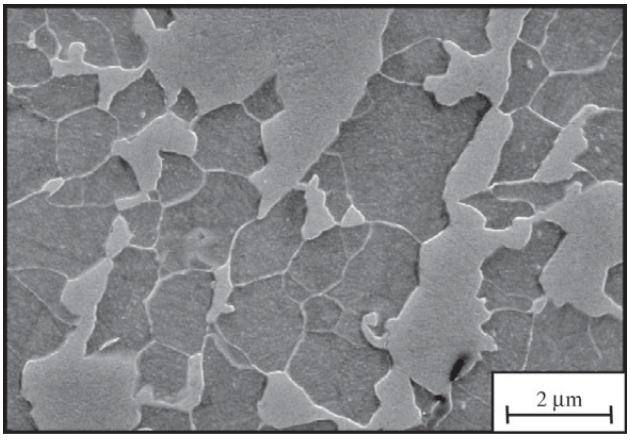

(b)

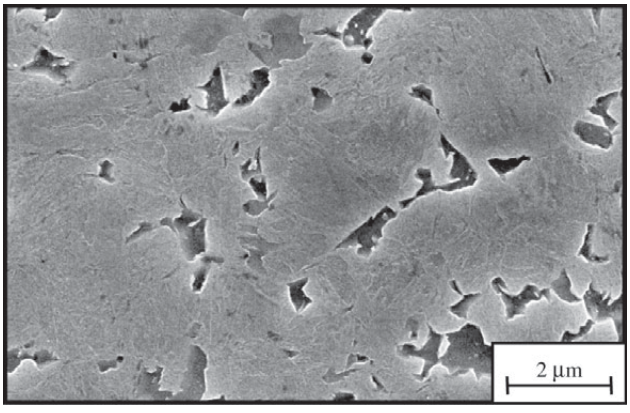

(c)

Figure 8. Microstructural evolution during the transformation of ferrite into austenite for samples deformed at 750 °C after a 3 min holding time. a) Sample strained to ε = 0.5; b) Sample strained to ε = 0.85; c) Sample strained to ε = 3.0.

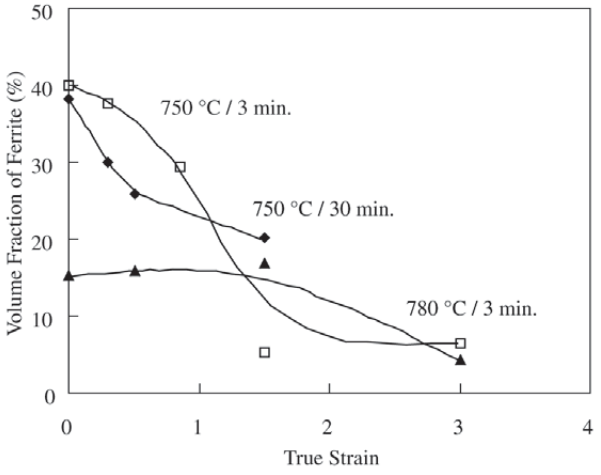

Figure 9. Evolution of the volume fraction of ferrite with deformation in the samples strained at 750 °C (3 and 30 min) and at 780 °C (3 min).

shapes and stress levels. These differences reveal the strained ferrite and pearlite, ferrite and austenite, and austenite structures and, hence, the evolution of the phase transformation during plastic deformation under warm conditions. Figs. 7 and 8 indicate that the phase-transformation transition from the first to the second stage took place at 750 °C after 1 min holding time. At this point, the peak strain was displaced considerably from values under 0.2 to values exceeding 0.4 (Fig. 5). The slope of the work-hardening rate was reduced while the curve still maintained a linear shape (Fig. 6a).

The flow stress displayed a hump with little straining at lower temperatures, i.e., 700 °C and 720 °C. When pearlite and ferrite are strained together, the deformation behavior is far from being homogeneous; the partitioning of stress and strain in two-phase composite materials is rather complex. The larger part of the strain is carried by the softer alpha phase, while the stress is concentrated in the harder cementite phase. The large volume fraction of pearlite leads to a great hardening with increasing strain. The extensive flow-softening region observed after the peak stress can be associated with the evolution of the first stage of the transformation. Although both constituents remained unaltered until a higher straining was reached, as shown in Fig. 7b, analyzing the pearlitic regions under higher magnification revealed that the cementite lamellae were no longer continuous after straining above the peak stress. Therefore, the downward shift in the stress level after the peak may be associated with spheroidization and/or breakage of the pearlitic cementite lamellae[13].

After complete dissolution of pearlite, e.g., after a 3 min holding time at 750 °C, the deformation is applied in a microstructure composed of ferrite and austenite (Fig. 8a). When these phases are deformed together, strain concentration occurred in the softer alpha phase at the onset of straining[14]. The shape of the flow stress curve changed and the peak stress was observed only after application of higher straining. Fig. 6a indicates the linear drop of the work-hardening rate and also certain dynamic softening. The literature reports that this behavior is caused by dynamic recovery[15,16]. Confirming this hypothesis, Fig. 8a shows the presence of subgrains in the strained ferritic grains.

As the deformation proceeded, austenite nuclei in ferrite grow and tend to consume all the ferrite. Figure 9 indicates that the volume fraction of ferrite decreased continuously, tending toward equilibrium values at $\varepsilon = 3.0$, independently of the testing conditions. Bearing in mind that these experiments were carried out at a strain rate of 1 s^{-1}, the time spent to complete the test and, thus, to reach phase transformation, was close to 3 s. Comparing this time with that elapsed for the reaction conducted without straining, longer times were required for static conditions, as reveals Fig. 2. At 750 °C, for instance, the volume fraction of austenite did not reach the same level at holding times as long as 1800 s.

The acceleration of ferrite to austenite transformation may be related to the increase of the stored strain energy caused by deformation. When both phases are deformed together, the ferritic phase concentrates deformation and the dynamic recovery mechanism is more effective in this phase. After some straining, a structure of subgrains is formed in the ferritic grains. Furthermore, the boundaries are able to store sufficient strain energy to provide favorable sites for nucleation of austenite. Therefore, the energy recovered through the annihilation of subgrain boundaries represents a substantial net reduction in the energy barrier to austenite nucleation, promoting a strain-induced dynamic transformation.

5. Conclusions

Samples deformed in and close to the intercritical domain after different holding times presented flow stresses of several shapes and degrees of stress. These differences revealed the strained structures and, therefore, the evolution of phase transformation during plastic deformation under warm conditions.

When pearlite and ferrite were strained together, the flow curves showed rapid work hardening to a hump, followed by an extensive flow-softening region. The large volume fraction of pearlite leads to a higher degree of hardening during the early stages of deformation. The downward shift in the level of stress after the peak may be associated with spheroidization and/or breakage of the pearlitic cementite lamellae.

After the pearlite consumption, the austenite and ferrite were deformed together, and a subgrain structure was

developed in the ferritic grains after some straining. The boundaries of these subgrains stored sufficient strain energy to become favorable sites for the nucleation of austenite. The transformation of ferrite into austenite was no longer controlled by the austenite growth only. The new process of intragranular nucleation accelerated the phase transformation, promoting strain-induced dynamic transformation.

Acknowledgements

The financial support of the Brazilian research funding agencies FAPESP and CNPq is gratefully acknowledged.

References

1. Garcia, C.I.; DeArdo, A.J. *Metall. Trans. A.*, v. 12A, p. 521-529, 1981.
2. Caballero, F.G.; Capdevila, C.; García de Andrés, C. *Metall. Mater. Trans. A.*, v. 32A, p. 1283-1291, 2001.
3. Speich, G.R.; Demarest, V.A.; Miller, R.L. *Metall. Trans. A.*, v. 12A, p. 1419-1428, 1981.
4. Hillet, M.; Nilsson, k.; Torndahl, L.E. J. *Iron Steel Inst.*, v. 209, p. 49-66, 1971.
5. Manohar, P.A.; Chandra, T.; Killmore, C.R. *ISIJ Int.*, v. 36, p. 1486-1493, 1996.
6. Liu, X.; Solberg, J.K.; Gjengendal, R. *Mater. Sci. Technol.*, v. 12, p. 345-350, 1996.
7. Niikura, M.; Fujioka, M.; Adachi, Y.; Matsukura, A.; Yokota, T.; Shirota, Y.; Hagiwara, Y. *Mater. Proc. Technol.*, v. 117, p. 341-346, 2001.
8. Hurley, P. J.; Hodgson, P. D. *Mater. Sci. Eng.*, v. A302, p. 206-214, 2001.
9. Hurley, P. J.; Muddle, B. C.; Hodgson, P.D. *Metall. Mater. Trans. A.*, v. 32A, p. 1507-1517, 2001.
10. Poliak, E.I.; Jonas, J.J. *Acta Mater.*, v. 44, p. 127-136,1996.
11. McQueen, H.J.; Ryan, N.D.; Evangelista, E. *Mater. Sci. Forum*, v. 113-115, p. 435-440, 1993.
12. Medina, S.F.; Hernandez, C.A. *Acta Mater.*, v. 44, p. 165-171, 1996.
13. Lourenço, N.J.; Jorge Jr., A. M.; Rollo, J.M.A.; Balancin, O. *Mater. Res.*, v. 4, p. 149-156, 2001.
14. Balancin, O.; Hoffmann, W.A.M.; Jonas, J.J. *Metall. Mater. Trans. A.*, v. 31A, p. 1353-1364, 2000.
15. Jorge Jr., A.M.; Regone, W.; Balancin, O. *Mater. Proc. Technol.*, v. 142, p. 415-421, 2003.
16. Chu, D.; Morris Jr., J.W. *Acta Mater.*, v. 45, p. 2599-2610, 1996.